Journal of
GEOPHYSICAL RESEARCH

VOLUME 72 OCTOBER 1, 1967 No. 19

A Theory of Discrete VLF Emissions from the Magnetosphere

R. A. HELLIWELL

Radioscience Laboratory
Stanford University, Stanford, California 94305

Some of the spectral forms (e.g. 'inverted' hook) of discrete VLF emissions are not explained satisfactorily by present theories of generation based simply on gyroresonance between energetic streaming electrons and whistler-mode waves traveling in the opposite direction. An extension of the gyroresonance idea is proposed in which the *spatial variations* of the electron gyrofrequency and the Doppler-shifted wave frequency are matched. The coupling time between a resonant electron and the wave is then maximized, and hence the output wave intensity is maximized. Application of this condition leads directly to an expression for the time rate of change of emission frequency in terms of the location of the interaction region. An approximate analysis of the postulated interaction process leads to a theorem that states: The magnetic field intensity is limited to a value less than that at which the bunching time approximately equals the resonance time. When the input particle flux exceeds the value required to account for this limiting value of wave intensity, the interaction region drifts downstream. If the interaction begins on the falling-tone or 'upstream' side of the equator, positive drift carries the interaction across the equator into the rising-tone region, giving rise to the well known 'hook' shape. Reversal of the drift, resulting from wave damping or other factors, carries the interaction back across the equator, giving rise to the inverted hook, a shape not explained by previous theories. Combinations of positive and negative drifts can explain the principal emission forms. The triggering delay and offset frequency of artificially triggered discrete VLF emissions can be explained by the theory.

1. INTRODUCTION

The purpose of this paper is to develop a phenomenological theory of discrete (monochromatic) VLF emissions and to compare the theory with observations made on the ground. These emissions are observed between about 200 and 30,000 hz and consist of trains of waves having a sharply-defined center frequency that varies with time. A train of such waves typically contains hundreds or thousands of cycles of roughly constant amplitude. The observational evidence has led to the suggestion that they are produced in the magnetosphere near the geomagnetic equator by trapped energetic electrons. These electrons couple energy to whistler-mode waves through a feedback mechanism based on cyclotron resonance. The generated waves then travel to earth in field-aligned ducts.

An understanding of the source of discrete VLF emissions is needed for several reasons. First, the background noise in VLF communications may at times be set by discrete VLF emissions, and hence an ability to predict their intensity would be useful. Second, since discrete VLF emissions exhibit several measurable characteristics, it may be possible to use some or all of them to describe the properties of the interacting electrons. This would fill an important need since most data on energetic electrons are now obtainable only with the aid of rockets and satellites. Furthermore the time variations of the properties of trapped electrons in a limited region of space, such as a whistler

duct, are difficult to measure with space vehicles. One of the outstanding problems associated with trapped electrons is the cause, or causes, of their precipitation into the ionosphere. Precipitation associated with the large-signal feedback process discussed in this paper may be significant, and would be complementary to *Kennel and Petschek* [1966], which relates electron pitch-angle diffusion to wideband whistler-mode noise. Finally, we note that the properties of emissions also depend on the density of the background thermal electrons and hence may contribute to the measurement of local electron density.

This paper is divided into four main parts. Following the introduction, in section 2, is a review of previous attempts to explain discrete VLF emissions. None of the theories has been able to explain both the narrow bandwidth and the variable frequency of discrete VLF emissions without making one or more unsupported assumptions.

The present theory is outlined in section 3. Using the concepts of cyclotron resonance and feedback, a model of the generation process is developed that exhibits certain novel features. It is in effect a kind of drifting cyclotron oscillator. It is shown that change of frequency with time is a direct result of feedback in a region of spatially varying gyrofrequency. Phase bunching of the input resonant electrons by the output wave provides the transverse current required to drive the oscillator. It is further demonstrated that the oscillation is self-limiting in amplitude. Amplitude limiting leads to spatial drift of the region of oscillation, the velocity of which depends on the flux of resonant electrons. A necessary condition on the velocity of this drift that must be satisfied by observed emissions is stated.

Finally, comparisons of the theory with observations are made in section 4. It is shown that the theory can account for the observed spectral forms including reversals in their slopes. The necessary condition on drift velocity is found to be amply satisfied in the case of a typical triggered hook. The characteristics of artificially triggered VLF emissions are interpreted in terms of the theory, including dependence of triggering on signal duration, triggering delay, and the 'offset' frequency. The paper concludes with a qualitative explanation of the mechanism of termination of an emission in terms of the effects of wave absorption and variation of particle flux with frequency.

2. Previous Work

The first attempt to explain the spectral shapes of discrete VLF emissions was based on an analogy with a traveling wave tube amplifier [*Gallet and Helliwell*, 1959]. In this mechanism, ambient whistler-mode noise provided the input signal that was amplified by an assumed small bunch of trapped electrons whose streaming velocity equaled the longitudinal component of the wave velocity. However, the existence of the postulated bunch of electrons was not demonstrated.

The next suggestion also postulated bunches of electrons, but assumed that they radiated Doppler-shifted, backward-traveling whistler-mode waves [*Dowden*, 1962*b*]. Several spectral forms were explained by this mechanism. It was shown, for example, that rising tones could be produced by an electron bunch traveling down a magnetic line of force (because the local gyrofrequency was increasing) and, conversely, falling tones by a similar bunch traveling up a line of force. When a bunch crossed the magnetic equator a 'hook' could be produced, but the quantitative agreement between experiment and theory in this case was questioned [*Brice*, 1962]. Dowden's theory also failed to explain long-enduring quasi-constant tones [*Brice*, 1964*a*]. It will be demonstrated later, however, that the Dowden mechanism is a limiting case of the present theory. Still another mechanism employing particle bunches was suggested by *Ellis* [1964] and is based on anomalous Doppler radiation.

The bunch theory was also applied to the phenomenon of periodic emissions, which consist of a series of similar equally spaced discrete emissions [*Dowden*, 1962*b*]. These emissions were observed to be in antiphase at conjugate points, and this circumstance was cited in support of the idea that they were produced symmetrically on either side of the equatorial plane by a bunch of electrons echoing between its mirror points. It was shown that the spacings between successive discrete emissions were comparable with typical values of the bounce periods of the resonant electrons.

However, in another study of periodic emis-

sions it was found that the period of the emission was equal to the whistler-mode echoing period for the path [*Helliwell*, 1963; *Helliwell and Brice*, 1964]. In addition it was observed that a periodic emission often originated in a whistler. These facts led to the suggestion that each emission was triggered by the whistler-mode echo of the previous emission, which acted to organize the phases of resonant particles so as to cause them to radiate coherently. Then it was discovered that discrete emissions could be triggered repeatedly by man-made signals from the ground [*Helliwell et al.*, 1964]. This fact was not compatible with a mechanism dependent on mirroring particle bunches. It was concluded, therefore, that the conditions for generation were omnipresent and that a different mechanism must be found.

The transverse resonance instability was suggested by *Brice* [1963] to avoid the difficulties of the bunch theory mentioned above. Although this mechanism is based on the same resonance condition employed by Dowden, it differs fundamentally from Dowden's theory in that it depends on feedback between the backward traveling waves and the forward traveling electrons. It was pointed out by Brice that feedback allows the interaction region to remain fixed in space, so that the mechanism can be viewed as a kind of backward-wave oscillator. This feedback process is the starting point for the present analysis.

The importance of phase coherence was also recognized by *Hansen* [1963] who suggested that a cyclotron emission would tend to be triggered by a strong whistler-mode wave in a region where the rate of change of electron gyrofrequency equaled that of the Doppler-shifted wave frequency. Although this idea is closely related to the present theory, it was not developed quantitatively and was not applied to the maintenance of the oscillations themselves.

Support for Brice's hypothesis was obtained by *Bell and Buneman* [1964] who calculated the conditions for the growth of the transverse resonance instability and showed their compatibility with the experimental data on artificially triggered emissions. Although the transverse resonance instability explained the presence of an oscillation, it did not of itself predict the spectral forms of discrete emissions.

Other studies of wave-particle interaction involving cyclotron resonance have emphasized incoherent interaction [e.g., *Kennel and Petscheck*, 1966; *Cornwall*, 1965]. In this approach it is assumed that the displacement of particles by the wave is small compared with the wavelength of the perturbing field. On the other hand the mechanism outlined in the present paper depends primarily on phase bunching of electrons, which involves significant longitudinal displacements of the resonant electrons.

3. Theory

It must be emphasized at the start that the following analysis is unrefined and is intended only to establish the reasonableness of the model.

In carrying out the analysis, several common assumptions are made. Propagation of the generated waves is assumed to be controlled by the ambient thermal (cold) plasma, and the direction of propagation is taken parallel to the static magnetic field. Collisions are neglected. The lateral extent of the interaction is assumed large so that the waves can be assumed plane.

The main point of departure in the present analysis is the assumption that the spatial variations of the electron gyrofrequency and the Doppler-shifted wave frequency must be matched. This is called the 'consistent-wave' condition and insures that the time during which an electron is in resonance with the generated wave will be a maximum, and hence the energy delivered to the wave can be expected to maximize also. Application of the consistent-wave condition leads directly to a description of the frequency-time variation as seen by a fixed observer.

It is then assumed that the oscillation takes place in a region that may be fixed in space or may drift forward or backward. This is called the 'interaction' region. Within the frame of the interaction region, the wave amplitude and the transverse electron current vary with position but not with time. Thus at any point within the interaction region we see a constant wave amplitude and a constant transverse electron current. The transverse electron current depends on the phase bunching produced by the magnetic field of the wave, while the wave in turn is radiated by the transverse currents.

Using a simple phasing criterion, the length of the resonance region is estimated, from which

the bandwidth is determined. Then the bunching time is found in terms of the wave magnetic field intensity and the transverse component of the electron velocity. Transverse current density is then calculated for a particular velocity distribution on the assumption that the pitch-angle distribution is isotropic, the phases of the input transverse velocities are random, and the concentration of electrons is constant over the small range of parallel velocities involved. Neglecting the effect of wave amplitude on the bandwidth, it is found that the wave amplitude stabilizes approximately at the value for which the bunching time equals the resonance time.

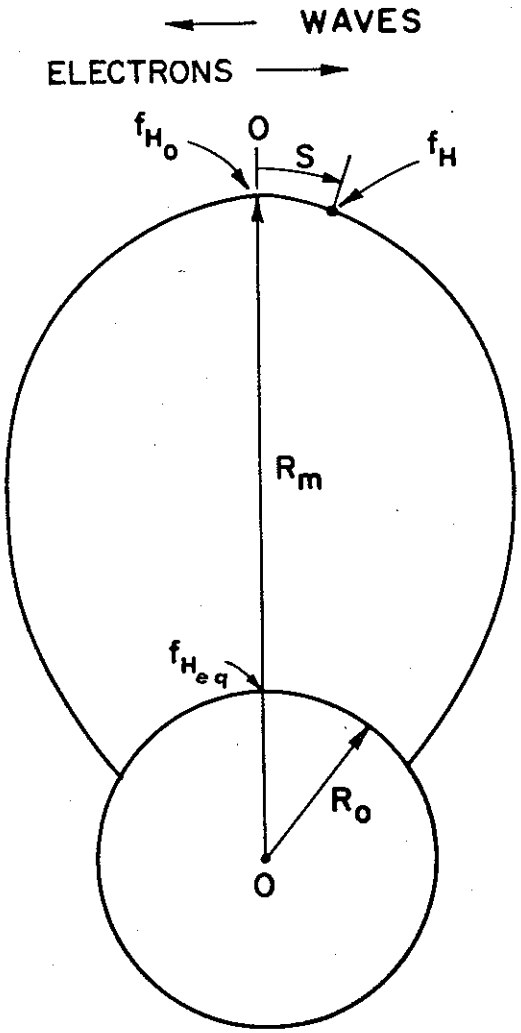

Fig. 1. Sketch illustrating notation for parameters of the interaction region.

Application of the limiting amplitude idea and of conservation of energy leads to the necessity for drift of the interaction region, from which particle flux and oscillator efficiency are deduced. This completes the first-order description of the drifting cyclotron oscillator model.

Frequency change. The consistent wave condition requires that the spatial variations of electron gyrofrequency and Doppler-shifted wave frequency be equal to first order. Consider a region near the equatorial plane. Let S be the distance measured from the equatorial plane to the interaction point in the streaming direction (see Figure 1). Then the wave frequency is given by the well-known relation

$$f = f_H \frac{v_p}{v_p + v_\parallel} \tag{1}$$

and its variation by

$$df = f\left(\frac{df_H}{f_H} + \frac{dv_p}{v_p}\right) - \frac{f^2}{f_H v_p}(dv_p + dv_\parallel) \tag{2}$$

where

f_H = electron gyrofrequency.
v_p = wave phase velocity, measured in the negative S direction.
$v_\parallel$ = parallel component of electron velocity, measured in the positive S direction.

Before proceeding to the details of the consistent wave calculation, we shall describe the relevant parameters. The paths of propagation are aligned with the earth's field, and the refractive index is assumed much larger than unity. Then it is easily shown [*Helliwell*, 1965] that the phase and group velocities are given, respectively, by

$$v_p = c\frac{f^{1/2}(f_H - f)^{1/2}}{f_N} \tag{3}$$

and

$$v_g = 2c\frac{f^{1/2}(f_H - f)^{3/2}}{f_N f_H} \tag{4}$$

where

$c = 3 \times 10^8$ m/s.
f_N = plasma frequency.

The variation of the phase velocity is found from (3) to be given by

$$dv_p = \frac{c}{2f_N}\left[\frac{(f_H - 2f)\,df + f\,df_H}{f^{1/2}(f_H - f)^{1/2}}\right] \tag{5}$$

Using (1), and (3), it is readily shown that the parallel velocity of a resonant electron is given by

$$v_{\parallel} = \frac{c}{f_N} \frac{(f_H - f)^{3/2}}{f^{1/2}} \tag{6}$$

Using (4) and (6) we have

$$v_o/v_{\parallel} = 2(f/f_H) \tag{7}$$

The electron concentration near the equator is assumed to be independent of latitude. Numerical values will be taken from Angerami's data for moderately disturbed magnetic conditions [*Angerami*, 1966].

The static magnetic field is assumed to be that of a centered dipole. Since its magnitude is given by a rather cumbersome function of distance along the line of force, an approximation will be used. It is readily shown that the gyrofrequency near the equator is given by

$$f_H = f_{H0}\left(1 + \frac{4.5S^2}{R_m{}^2}\right) = f_{H0}\left[1 + \frac{4.5S^2}{R_0{}^2}\left(\frac{f_{H0}}{f_{Heq}}\right)^{2/3}\right] \tag{8}$$

and its variation by

$$df_H = 9\,\frac{f_{H0}}{R_m{}^2}\,SdS \tag{9}$$

where

R_0 = radius of earth (6370 km).
R_m = distance to top of path from earth's center.
S = distance from top of path to point of measurement (positive to right of equator, negative to left).
f_{H0} = gyrofrequency at top of path.
f_{Heq} = gyrofrequency at earth's surface on equator = 880 khz.

The notation for the parameters of the interaction region is illustrated in Figure 1.

Finally, we will need the variation of $v_{\parallel}$, the streaming velocity of the electrons. This is controlled primarily by the static magnetic field, since the energy exchanged between particle and wave is always a small fraction of the total kinetic energy of the particle. Accordingly the effect of the wave on $v_{\parallel}$ is neglected, except in the bunching calculation.

According to the first adiabatic invariant, $\sin^2 \alpha/f_H$ = constant, where α is the pitch angle of the electron. The parallel component of electron velocity is then given by

$$v_{\parallel} = v\left(1 - f_H \frac{\sin^2 \alpha_0}{f_{H0}}\right)^{1/2} \tag{10}$$

and its variation by

$$dv_{\parallel} = -\frac{v_{\parallel}}{2f_H}(\tan^2 \alpha)\, df_H \tag{11}$$

where

v = speed of electron.
α_0 = pitch angle at the equator.
α = pitch angle at center of interaction region.

We are now ready to consider the variation of frequency with time. First we need to clarify certain features of the model. It is assumed that the interaction region is many wavelengths long and that within the interaction region the wave amplitude decreases smoothly from its maximum value to zero. A schematic drawing of the interaction region is shown in the upper part of Figure 2, in terms of a Cartesian component of one of the wave field vectors versus distance. It is assumed that the gyrofrequency is increasing with S, corresponding to a position on the right-hand side of the equator in the sketch of Figure 1. As mentioned earlier, the variation of wave frequency with distance must be such that those electrons that contribute most to growth of the wave remain in resonance for the longest time. It should be noted that each interacting electron resonates for a limited time; new electrons flow into the interaction region at a rate that depends on the drift velocity of the interaction region. It will be recalled that in Dowden's theory [*Dowden*, 1962*a*] each discrete emission was generated by a single bunch of electrons that radiated a wave of changing frequency as it traveled along a line of force. Dowden's theory is simply a limiting case of the present theory in which the drift velocity of the interaction region equals the particle streaming velocity.

To obtain a quantitative expression for the change of frequency with time, consider the sketch in the lower part of Figure 2, showing a small section of the interaction region at three

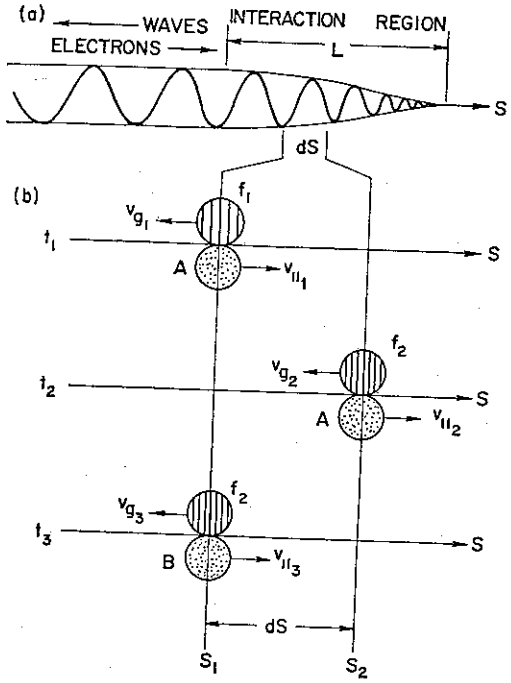

Fig 2. Sketch showing: (*a*) variation of a wave field component with position in the interaction region, (*b*) relation of wave packets and resonant electrons between two closely spaced points within the interaction region.

instants of time, t_1, t_2, and t_3. At time t_1, and position S_1, a wave packet at frequency f_1 resonates with a group of electrons, labeled A, traveling to the right at velocity $v_{\parallel 1}$. When these electrons reach position S_2, they have a different gyrofrequency and a different streaming velocity $v_{\parallel 2}$ and hence resonate with a wave packet of different frequency f_2. The wave packet at frequency f_2 then travels back to position S_1 where it resonates with a new group of electrons, labeled B, traveling to the right at velocity $v_{\parallel 3}$. An observer stationed at position S_1 then sees a change in frequency $f_2 - f_1$ in an interval of time $t_3 - t_1$.

The change in frequency $df = f_2 - f_1$ over the path segment dS can be found in terms of the wave frequency and the parameters of the medium by substituting (3), (5), (6), and (11) in (2), getting

$$df = \frac{3\lambda}{1+2\lambda}\left[1 + \frac{(1-\lambda)}{3}\tan^2\alpha\right] df_H \quad (12)$$

where $\lambda = f/f_H$.

The elapsed time $dt = t_3 - t$, between the arrival at position S_1 of the wave packet at frequency f_1 and that at frequency f_2 is simply

$$dt = dS\left(\frac{1}{v_\parallel} + \frac{1}{v_g}\right) \quad (13)$$

where

$v_\parallel$ = average parallel velocity of electrons traveling between S_1 and S_2.

v_g = average group velocity of wave packet traveling from S_2 back to S_1.

The rate of change of frequency with time, found by dividing (12) by (13), is given by

$$\frac{df}{dt} = \frac{df_H}{dS}\left(\frac{v_g}{1 + v_g/v_\parallel}\right)\left(\frac{3\lambda}{1+2\lambda}\right) \cdot\left[1 + \frac{(1-\lambda)}{3}\tan^2\alpha\right] \quad (14)$$

The dependence of df/dt on S can be obtained by substituting (9), and v_g and $v_g/v_\parallel$ can be expressed in terms of the parameters of the medium by substituting (4) and (7). Furthermore, the values of S of interest are small so we can put $f_H = f_{H_0}$, giving finally

$$\frac{df}{dt} = K_1 S\lambda^{3/2}\frac{(1-\lambda)^{3/2}}{(1+2\lambda)^2} \cdot\left[1 + \frac{(1-\lambda)}{3}\tan^2\alpha\right] \quad (15)$$

where

$$K_1 = \frac{54cf_{H0}^{\ 2}}{R_m^{\ 2}f_N}\ \mathrm{m^{-1}\ sec^{-2}}$$

To illustrate the nature of (15) it is assumed for simplicity that $\alpha = 0$ since the correction term in the brackets is less than 0.1 for our working value (30°) of the pitch angle (derived later). Then the quantity $(1/K_1S)(df/dt) = \lambda^{3/2}([1-\lambda]^{3/2}/[1+2\lambda]^2)$ is a measure of the slope of an emission generated at a *fixed* location, and is plotted in Figure 3. The maximum slope is seen to occur at $\lambda = 0.32$, which is close to the nose frequency (typically near 0.4 λ). Thus we might expect the slope to increase or decrease with frequency, at frequencies respectively well below or well above the nose. However the drift of the interaction region affects the variation of slope with time, as discussed below, and hence it is not possible to

predict the variation of slope with time, using only (15).

Length of resonance region. As electrons enter the interaction region they begin to drift toward their 'stable' point under the influence of the longitudinal drift force, which is proportional to the perpendicular velocity of electrons and the wave magnetic field intensity. After significant bunching has been produced these electrons supply energy to the wave until they eventually become debunched as a result of the spread in the drift velocities. The downstream limit of the interaction region is marked by the point where both the transverse current and the wave intensity go to zero. It is clear that bunching and radiation occur throughout the interaction region, but that bunching dominates in the first half and radiation in the second half. To simplify the analysis we shall assume that bunching is confined to the first half of the interaction region and that the wave amplitude is constant within this region. During bunching it is assumed that the phase angle between the transverse velocity and the wave magnetic field must lie between $+\pi$ and $-\pi$, meaning that the electron lies within the central potential well of the wave. This central potential well is called the 'resonance region,' and its length is taken to be one-half the length of the interaction region.

Now consider a single test electron approaching the interaction region. Before it enters the central potential well of the wave, the electron's relative phase changes so rapidly that the wave amplitude remains essentially constant over 2π radians of phase change. Hence the *average* exchange of energy between wave and particle is small and can be neglected to first order. Bunching occurs mainly within the resonance region whose limits are the points where the phase is shifted $\pm\pi$ radians with respect to the phase at the center. It is within this region that the longitudinal force causes all resonant particles to drift toward a common stable point; after passing the stable point they become debunched. The debunching time is equal to the bunching time, in accordance with our assumption that the interaction length is twice the resonance length.

To find the resonance length, we calculate the difference in phase between the electron velocity and the magnetic field of the wave as a function of position with respect to the center of the resonance region, where the electron transverse velocity is antiparallel to the magnetic field of the wave. To simplify the analysis we shall calculate the 'unperturbed' phase that results when we neglect the change in phase caused by wave-induced longitudinal drift. In effect we consider only those resonant electrons whose longitudinal drift is negligible. The unperturbed phase shift can be found by integrating over time the difference between the gyrofrequency of the electron and the Doppler-shifted wave frequency seen by the electron. The gyrofrequency is given by (8), and the Doppler-shifted wave frequency as seen by the electron at position S is given by $f' = f_{H1} + \Delta f'$, where f_{H1} is the gyrofrequency at S_1, the center of the resonance region, and $\Delta f'$ is the change of f' between S_1 and S. The variation term $\Delta f'$ depends on df/dt at S_1 the group delay of the wave packet in traveling from S_1 to S, and the phase velocity (which changes with S because both f and f_H vary with S).

The analysis of the general case is rather involved and will be omitted in this first-order analysis. Instead the center of the resonance region will be taken on the equator so that $df/dt = 0$. Then the Doppler-shifted wave frequency as seen by the electron at point S is found from (1) to be given approximately by

$$f' = \left(1 + \frac{v_\parallel}{v_p}\right) f \qquad (16)$$

The variation of $v_\parallel$ for a given electron will be taken to be much less than the variation of

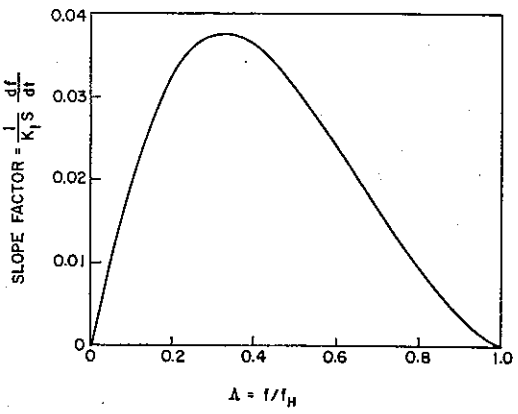

Fig. 3. Slope factor $(1/K_1S)(df/dt)$ for emissions generated at a fixed location.

v_p, so that we may assume $v_\parallel$ to be constant at its equatorial value. Then using (3), (6), and (8) in (16), we find that

$$f' = f_{H0}\left[1 - \frac{1}{2}\left(4.5\frac{S^2}{R_m^2} + \cdots\right)\right] \quad (17)$$

Subtracting (17) from (8) we have,

$$\Delta f = \frac{13.5}{2} f_{H0}\left(\frac{S}{R_m}\right)^2 \quad (18)$$

The differential phase shift is $d\theta = 2\pi\Delta f dt$, and since $v_\parallel dt = ds$, the total phase shift between the equator and S is given by

$$\theta = 2\pi \int_0^S \frac{\Delta f\, ds}{v_\parallel}$$

which is integrated to give

$$\theta = \frac{4.5\pi f_{H0}}{R_m^2 v_\parallel} S^3 \quad (19)$$

from (19) we find that

$$S = \left(\frac{\theta R_m^2 v_\parallel}{4.5\pi f_{H0}}\right)^{1/3} \quad (20)$$

which gives the distance from the center of the resonance region to the point where the phase of the unperturbed electron velocity has advanced θ radians with respect to the phase of the magnetic field of the wave. Putting $\theta = \pi$ in (20) and multiplying the result by 2, we find that the total length of the resonance region is

$$L = 2\left(\frac{R_m^2 v_\parallel}{4.5 f_{H0}}\right)^{1/3} \quad (21)$$

This can be expressed in terms of the wave frequency and the parameters of the medium by substituting (6) and noting that $f_{H0} = f_{Heq}(R_0/R_m)^3$, where $f_{Heq} = 8.8 \times 10^5$ hz and $R_0 = 6370$ km. The resonance length is then

$$L = 2\left[\frac{R_0^2}{4.5 f_{H0}}\left(\frac{f_{Heq}}{f_{H0}}\right)^{2/3}\frac{c}{f_N}\frac{(f_{H0} - f)^{3/2}}{f^{1/2}}\right]^{1/3} \quad (22)$$

$$= 5.85 \times 10^5 \frac{(1-\lambda)^{1/2}}{f_N^{1/3} f_{H0}^{2/3} \lambda^{1/6}} \text{ km}$$

where frequency is expressed in hz.

The variation of the resonance length L with wave frequency calculated from (22) is shown in Figure 4 for $f_N = 180$ khz, $f_{H0} = 13.75$ khz ($R_B = 4$), and $f_{H0} = 32.6$ khz ($R_B = 3$). It is seen that the resonance length depends mainly on f/f_{H0} and has values between roughly 1000 and 2000 km for the frequencies of principal interest. The number of wavelengths in the resonance region is usually large. For example, for the model used in Figure 4, with $R_B = 3$ and $f = 16.3$ khz ($\Lambda = 0.5$), the wavelength is readily found to be 1.67 km. Since the resonance length from Figure 4 is 810 km, the number of wavelengths is 485.

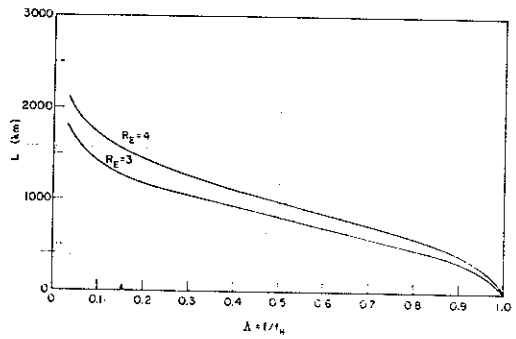

Fig. 4. Interaction length versus normalized wave frequency for $R_B = 3$ and $R_B = 4$.

Bandwidth. Closely related to the resonance length is the bandwidth of the radiation. It is assumed that the resonance region is centered on the equator so as to simplify the analysis. This is justified by the fact that the observed bandwidth is roughly independent of df/dt, and hence of the position of the interaction region. The variation of electron gyrofrequency over the interaction distance is one source of frequency spreading; this type will be called 'gyrofrequency broadening.' Because the transverse current shows a $\sin^2$ variation with distance, the contributions to the current at the beginning and end of the interaction region are small. We shall assume that the band limits correspond to the half-current points so that the corresponding length equals the resonance length. The amount of gyrofrequency broadening is then the maximum difference between the gyrofrequency and the Doppler-shifted wave frequency occurring within the resonance region. It is found by substituting $L/2$ for S in (18), and is given by

$$(\Delta f)_H = 1.7 f_{H0}\left(\frac{L}{R_m}\right)^2 \quad (23)$$

As an example of the magnitudes to be expected take $f_{H0} = 32.6$ khz ($R_B = 3$), $\Lambda = 0.5$, and $R_m = 19{,}100$ km. Then from Figure 4, $L = 810$ km, and (23) gives a bandwidth of 100 hz.

The spread in streaming velocities around the resonance value is the other source of frequency spreading; this type will be called 'Doppler broadening.' Off-resonance electrons will remain in the central potential well for a shorter time and hence will have shorter interaction lengths. For the small bandwidths involved, the frequency deviation remains approximately constant throughout the interaction region since off-resonance electrons see nearly the same variation of Doppler-shifted wave frequency with distance. The contribution that an off-resonance electron makes to the transverse current is assumed to go to zero when its phase with respect to the bunched resonance electrons exceeds $\pm\pi/2$ radians. The total bandwidth due to Doppler broadening over a resonance length L_Λ is then

$$(\Delta f)_D = v_\parallel / L_\Lambda \tag{24}$$

The maximum value of L_Λ is, of course, the resonance length at the resonant frequency. Thus if we let $L_\Lambda = L$, the corresponding bandwidth $(\Delta f)_D$ is just the reciprocal of the resonance time $(L/v_\parallel)$. A typical value of $(\Delta f)_D$ is $(4 \times 10^4$ km/sec$)/1000$ km $= 40$ hz, corresponding to a resonance time of 25 msec. At greater values of $(\Delta f)_D$, the resonance distance L_Λ is reduced. Hence the required $v_\perp$ must increase to make the bunching time equal the resonance time. As $v_\perp$ increases, $J_\perp$ drops, which, together with the drop in L_Λ, causes the contribution to the wave to decrease rapidly. The contribution of electrons whose resonance length is less than L is assumed small and will be neglected. Therefore the bandwidth due to Doppler broadening can be taken as $v_\parallel/L$. Then, letting $f_H = f_{H0}$ and substituting (6) and (22), (24) becomes

$$(\Delta f)_D = \frac{0.51 f_{H0}^{14/9}}{f_N^{2/3}} \frac{(1-\lambda)}{f^{1/3}} \tag{25}$$

The total bandwidth in this simple model is then given by the sum of (23) and (25).

Bunching time. As resonant electrons flow through the interaction region, they experience a longitudinal force given by

$$F_m = q v_\perp B_w \sin \frac{2\pi z}{\lambda} \tag{26}$$

where

q = particle charge.
$v_\perp$ = transverse velocity of charged particle.
B_w = magnetic field of wave.
z = longitudinal displacement from the 'stable' point.
λ = wavelength.

As time progresses each electron within the resonance region drifts toward its 'stable' point, at which $F_m = 0$. The drift velocity depends on the initial phase angle. From (26) it is seen that the relative longitudinal motion of the electron is similar to that of a simple pendulum in that the time required to reach the stable point is approximately independent of the initial phase, except when the initial phase angle is large ($> \pi/2$). The solution of (26) leads to the complete elliptic integral of the first kind for the period of oscillation. We shall adopt the period for small angles, which is a usable approximation up to initial phase angles of $\pm\pi/2$. Electrons outside this range, constituting half of those available, do not contribute much to the current and will be neglected. For small angles $\sin(2\pi z/\lambda)$ can be replaced by $2\pi z/\lambda$ in (26) and a harmonic solution obtained. The bunching time is one-quarter of the period of this oscillation and is given by

$$T = \left(\frac{\pi m}{8q} \frac{\lambda}{v_\perp B_w}\right)^{1/2} \tag{27}$$

In this length of time each electron moves from its position at the entrance to the interaction region to its zero phase, or stable point, at which the transverse current reaches a maximum. As time increases beyond the bunching time the phases of the individual electrons separate, becoming random again at $2T$, if the wave amplitude remains constant. Thus in the case of a constant-amplitude wave there is, to first order, no average exchange of energy between electron and wave because each electron experiences a component of electric field in the direction of the transverse velocity that varies symmetrically about zero.

Current density. The phase bunching of electrons in the manner just described produces a spatial maximum in the transverse current

density; it is the transverse current that supplies the observed radiation. The magnitude of the transverse current depends on the concentration of charged particles, and on the magnitude and phasing of their transverse velocities. Little is yet known about the variation of concentration with velocity, but recent work by *Frank* [1966] is reasonably consistent with the assumption that the electron spectrum is proportional to v^{-5}. Assuming complete bunching of the resonant electrons, the peak transverse current is proportional to the electron flux. Then assuming an isotropic distribution of pitch angles, the transverse current density per unit pitch angle can be expressed by

$$J'_{\perp} = J'_{\perp \max} \cos^5 \alpha \sin^2 \alpha \text{ amps/m}^2 \text{ radian} \quad (28)$$

where $J'_{\perp max}$ = the maximum transverse current density per unit pitch angle. Using (28) the normalized transverse current is plotted in Figure 5 and is found to peak at $\alpha_{max} = 30°$, which will be taken as the characteristic pitch angle for the interaction. (It is noted that usually the loss cone will have an angle of less than 10° and hence its neglect is not serious.) The corresponding characteristic value of the perpendicular velocity is then

$$v_{\perp} = 0.577 v_{\parallel} \quad (29)$$

Limiting wave intensity. The power radiated by the phased electrons depends on the length of the radiating region, the transverse current density, the transverse electric field, and the phase angle between the transverse current and the electric field. The power radiated is given

$$P = \int_0^{2L} J_{\perp} E \cos \theta \, dS \text{ watts/m}^2 \quad (30)$$

where

$J_{\perp}$ = transverse current density, amps/m².
E = intensity of circularly polarized electric field, v/m.
S = position within the interaction region, assumed to have a length $2L$ meters.
θ = phase angle between transverse current and wave electric field.

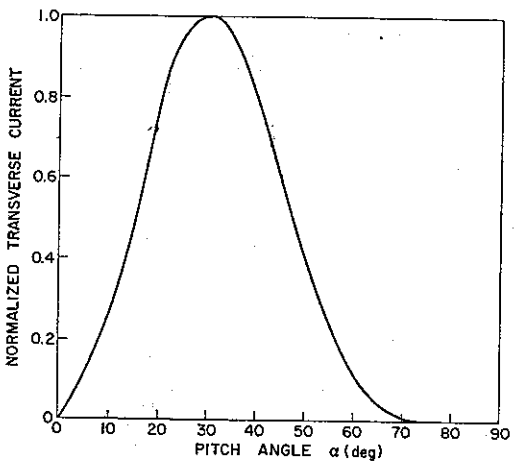

Fig. 5. Variation of normalized transverse current density with pitch angle.

Now suppose that an oscillation is started by a small-signal instability or by an external triggering signal. Then as the wave intensity increases, the bunching time diminishes according to (27). At first the bunching time is greater than the resonance time so that the current does not reach its maximum possible value before the partially bunched electrons leave the resonance region. For small fractions of the bunching time, (26) shows that the largest displacements of electrons occur where the initial phase angle is near $\pi/2$. Since the drift force is roughly constant for small displacement, these displacements vary roughly as the square of the time of exposure to the resonant wave field. The power per unit length along the static magnetic field increases as the square of the current and hence as the fourth power of the exposure time. The power required for a given bunching time also increases as the fourth power of the time since $B_w \propto 1/T^2$ from (27) and $P \propto B_w^2$. Thus we require some additional factor to make the input power rise faster than the required output power. This is provided by the increase (assumed small) in the width of the parallel velocity spectrum resulting from increased wave amplitude. Although the amount of this increase has not yet been calculated, it is sufficient to observe that initially at least it will cause the power output to increase with time raised to an exponent greater than 4. This insures that the postulated growth mechanism can indeed exist without the conditions for the small-signal transverse resonance instability having to be satisfied.

It is clear that when the bunching time is

reduced to the resonance time, the peak current ceases to increase, assuming constant $(\Delta f)_D$. Thus any further increase in B_w would reduce the bunching time without increasing the current, and hence the power output would drop according to (30). Even the maximum possible increase in $J_\perp$ due to an increase in $(\Delta f)_D$ would not be sufficient to compensate for the leveling off of the current produced by the resonance electrons and the reduction of the bunching time. Thus the maximum possible wave amplitude is approximately equal to the wave amplitude required to make the bunching time equal to the resonance time. Obviously more detailed calculations are required to establish its exact value. In the meantime, we shall adopt the following theorem: *Wave amplitude is limited to a value less than that at which the bunching time equals the resonance time.*

To find the limiting value of the wave magnetic field, we let the resonance time $L/v_\parallel$ equal the bunching time T and solve (27), obtaining

$$B_w = \frac{\pi}{8}\frac{m}{q}\frac{\lambda}{v_\perp}\frac{v_\parallel^2}{L^2} \tag{31}$$

which can be simplified further by using (22), (6), $\lambda = v_p/f$, (3), $v_\perp = v_\parallel \tan \alpha$, and putting $f_{H0} = f_H$, obtaining finally

$$B_w = K_2 \frac{f_{H0}^{13/9}(1-\Lambda)}{f_N^{4/3}\Lambda^{2/3}} \cot \alpha \text{ webers/m}^2 \tag{32}$$

where $K_2 = 5.8 \times 10^{-13}$, with frequency measured in hz.

Thus B_w is independent of the magnitude of particle flux, but does depend on the energy spectrum of the electrons through the factor cot α. It is also seen that B_w increases with decreasing wave frequency.

To obtain an estimate of the flux of resonant electrons required to produce the value of B_w given by (32), we need to know the spatial variation of the transverse current $J_\perp(S)$ and its phase angle with respect to the electric field. A simple approximate description of $J_\perp(S)$ can be found by noting in (26) that for small displacements from the stable point, the phase angle of the electron velocity varies sinusoidally with time, and hence with distance (since $v_\parallel \doteqdot$ constant). If we assume an equal population of electrons at all initial phase angles, then it is found that the transverse current varies with distance approximately as $(1 - \cos 2\phi)$, or as $\sin^2 \phi$, where $\phi = \pi S/2L$. Note that in this description the transverse current reaches a maximum in one resonance length, but that the current continues beyond this point, dropping to zero in one more resonance length. Thus the current is assumed to extend over a distance of $2L$, and therefore the phase angle between $\bar{E}$ and $\bar{J}_\perp$ will be assumed to vary from $\pi/2$ to π in this same distance. The phase at $S = 2L$ is equal to π to take account of the fact that power flows from the electrons to the wave, and a linear variation of phase with distance is assumed for simplicity. Then the power density radiated from a small slab of thickness dS is given by

$$dP = EJ_{\perp \max} \sin^2 \frac{\pi S}{2L} \cos \frac{\pi}{2}\left(1 + \frac{S}{2L}\right) dS \text{ watts/m}^2 \tag{33}$$

But $P = E^2/Z$, where $Z = 377/\mu$ ohms, so that (33) can be written with variables separated as

$$\int_{P\max}^{0} \frac{dP}{P^{1/2}} = -Z^{1/2} J_{\perp \max} \cdot \int_0^{2L} \sin^2 \frac{\pi S}{2L} \sin \frac{\pi S}{4L}\, dS \tag{34}$$

which can be integrated to give

$$P_{\max} = \left(\frac{16L}{15\pi}\right)^2 Z J_{\perp \max}^2 \tag{35}$$

The output wave power is $P_m = E_w^2/Z = B_w^2 Z/\mu_0^2$ so that (35) can be written

$$J_{\perp \max} = \frac{15\pi}{16\mu_0}\frac{B_w}{L} \text{ amps/m}^2 \tag{36}$$

A typical value for $J_{\perp\max}$ can be found by taking $\Lambda = 0.5$, $\alpha = 30°$, $R_B = 3$, and $f_N = 180$ khz. Then from Figure 4, $L = 810$ km and from (32) $B_w \approx 2.71 \times 10^{-13}$ webers/m^2, which can be substituted in (36) to give $J_{\perp\max} = 7.86 \times 10^{-13}$ amps/m^2. From (6) we get $v_\parallel = 2.72 \times 10^7$ m/s, and hence $v_\perp = 1.57 \times 10^7$ m/s. Since $J_{\perp\max} = Nqv_\perp$, the corresponding concentration of electrons in the transverse current stream is

$$N = \frac{7.86 \times 10^{-13}}{1.6 \times 10^{-19} \times 1.57 \times 10^7} \approx 0.31 \text{ m}^{-3}$$

Using (24), we estimate the Doppler broadening to be

$$\frac{2.72 \times 10^7}{810 \times 10^3} = 33.6 \text{ hz}$$

which corresponds to a fractional spread in parallel velocity of

$$2 \times \frac{33.6}{16.3 \times 10^3} \approx \frac{1}{240}$$

Since the total velocity of the resonant particles is about 3×10^7 m/s, their mean energy is 2.6 kev with a spread of 11 ev. The corresponding differential particle flux is then

$$\frac{3.1 \times 10^{-7} \text{ cm}^{-3} \times 3 \times 10^9 \text{ cm sec}^{-1}}{11 \text{ ev}}$$

$$= 85(\text{cm}^2 \text{ sec ev})^{-1}$$

a not unreasonable value.

The efficiency of the oscillator is readily calculated by dividing the ac power output by the dc power input supplied by the resonant electrons. The input power is simply $\frac{1}{2}N$ mv^3 and for the numbers used above is

$$P_{in} = 1.6 \times 10^{-19} \frac{\text{joules}}{\text{ev}} \times 2.6 \times 10^3 \text{ ev} \times 0.31 \text{ m}^{-3} \times 3 \times 10^7 \text{ m/s}$$

$$= 3.9 \times 10^{-9} \text{ w/m}^2$$

while the output power is

$$P_{out} = \frac{B_w^2 Z}{\mu_0^2} = \left(\frac{2.71 \times 10^{-13}}{4\pi \times 10^{-7}}\right)^2 \frac{377}{11}$$

$$= 1.6 \times 10^{-12} \text{ w/m}^2$$

The efficiency is therefore less than 0.1%. Such a low value means that the motion of the electron is not affected significantly by the electric field of the wave, thus validating our neglect of this factor in our approximate analysis of the motion of the resonant electrons. Furthermore a low value of efficiency means that a particular electron can undergo many successive interactions as it bounces between its mirror points before becoming significantly de-energized. On the other hand, electrons close to the loss cone will tend to be dumped following interaction since the electron pitch angle decreases when the electron transverse energy decreases [*Brice*, 1964*b*].

Drift of interaction region. Employing the theorem of the limiting intensity stated above, we obtain the magnitude of the magnetic intensity of the wave. The wave energy is convected away from the interaction region at the group velocity and must be supplied by the incoming electrons. If the input power from the streaming electrons is not exactly equal to the output wave power for a fixed position, then the interaction region will drift either downstream or upstream at a velocity such that input power equals output power.

With respect to the drifting interaction region, the output power is proportional to $v_g + v_i$, where v_i = drift velocity, taken positive in the electron streaming direction ($+S$), and v_g = group velocity of wave energy, taken positive in the wave direction ($-S$). Thus when the interaction region drifts backward at the wave group velocity ($v_i = -v_g$), no power flows out of the region and hence no input power is required.

The input power, on the other hand, is proportional to $v_\parallel - v_i$ and therefore decreases as v_i increases, becoming zero when $v_i = v_\parallel$. This limiting condition corresponds exactly to Dowden's 'particle bunch' theory of emission generation [*Dowden*, 1962*b*] and means that the same electrons remain in the interaction region, with the result that the average transfer of energy to the wave must go to zero. Thus we would expect the drift velocity to approach the parallel velocity of the resonant electrons only under conditions of very high particle fluxes. Furthermore, if the particle flux is sufficient to produce a detectable discrete emission, it is highly likely that it will exceed the value required for zero drift. Hence positive drifts can be expected.

From the energy conservation properties developed above, we can state the necessary condition that

$$-v_g < v_i < v_\parallel \qquad (37)$$

where $v_i = ds/dt$ (drift velocity of interaction region).

We have assumed no change in $df_\parallel/dS$ with time, but this may not always be justified, especially during periods of magnetic disturbance. Perturbations in magnetic field strength

P 4784 missing

propagating along the field would cause temporal changes in df_H/dS and hence in df/dt that would look like those caused by drift.

4. Comparison of Theory with Observations

Because of limitations of time and space, comparison of theory with experiment will be restricted to an interpretation of certain general features of emissions and a detailed analysis of one hook. The comparison appears sufficient to demonstrate that the theory accounts for the principal features of emissions. Extensive detailed comparisons will be reported at a later date.

Spectral shapes. For a falling electron energy spectrum, the equator is the most likely starting place for emissions, as pointed out by *Brice* [1964c], because the streaming velocity (see (6)) is minimum here, and hence the available particle flux is maximum. Since positive drift is expected, the emission slope will be positive, giving a predominance of rising tones, as observed. On the other hand, when the oscillation is initiated by a whistler with negative slope, then the starting point is likely to be on the upstream side of the equator. A positive drift then carries the interaction region across the equator into the region of rising tones. The result is an emission that first falls, then rises in frequency, as observed in the so-called 'hook.'

Finally, we observe that if the input flux becomes inadequate to sustain a positive drift, the interaction region will drift upstream. A rising tone is then followed by a falling tone, giving the so-called 'inverted hook' [*Helliwell,* 1965]. Changes of this kind could be caused by variations in the velocity spectrum or wave damping.

A peak in the electron velocity spectrum could cause a periodic movement of the interaction region between points on opposite sides of the equator, giving rise to an oscillating tone. Thus if we assume that the input particle flux increases as the frequency falls, we expect that at some frequency the drift velocity will become positive, and the interaction region will then move across the equator into the region of rising frequency. The resulting rise in frequency then leads to a reduction in flux, causing a reversal in drift velocity and the process repeats.

Some basic spectral forms and the corresponding locii of the interaction region are sketched in Figure 6. Each crossing of the equator corresponds to a maximum or minimum in frequency. It is noted that the last two forms, the inverted hook and the oscillating tone, have not been explained by previous theories.

Drift velocity. Application of (37) to observations of discrete emissions provides a useful test (necessary, but not sufficient) of the consistent-wave theory. The test procedure can be outlined as follows.

(1) Obtain values of f versus t from spectrogram.

(2) Find path latitude, using whistlers or echoing emissions.

(3) Correct $f(t)$ for dispersion, by subtracting one-half the one-hop whistler delay for the path. This correction assumes the interaction region is close to the equator.

(4) Plot df/dt from the corrected $f(t)$ curve.

(5) Compute and plot $s(t)$ for each chosen value of df/dt, using (15). Note that t is the time of *observation, at a fixed point,* and not the true time.

(6) Compute the true time at which the interaction region arrives at point S by subtracting from the observed time the wave group delay between the position S of the interaction region and the point of observation. The point of observation is somewhat arbitrary but should

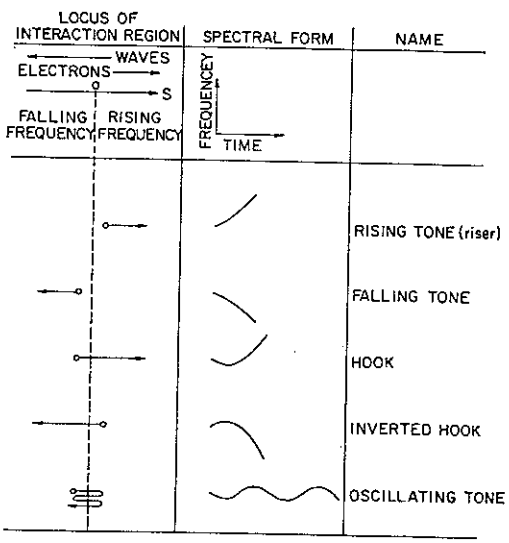

Fig. 6. Schematic diagram showing relation between the locus of the interaction region and the spectral form of the emission.

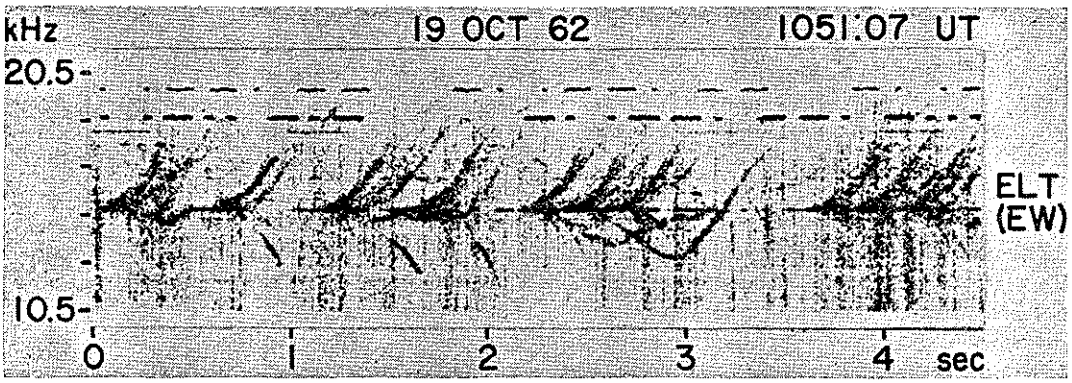

Fig. 7. Spectrogram showing hook at 2.5 sec triggered by NAA on 14.7 khz and recorded on Oct. 19, 1962, at 10h 51m 07s UT (taken from Fig. 7-66c, *Helliwell* [1965].

be upstream of all positions occupied by the interaction region.

(7) Plot a new curve of S versus true time and measure the drift velocity $v_t = ds/dt$ from this curve.

(8) Compare each value of v_t with the corresponding values of v_g and $v_\parallel$ to determine whether the necessary condition (37) is fulfilled.

The test outlined above has been applied to the triggered hook shown in Figure 7. The relevant parameters are listed in Table 1. Corrections for dispersion along the field-aligned path from the equator to the ground were small enough to be neglected (mainly because the hook frequencies were close to the 'nose' frequency).

The $f(t)$ curve for the hook as scaled from Figure 7 is plotted in Figure 8*a*. Since the correction for dispersion is negligible, Figure 8*a* is used directly to obtain df/dt, which is plotted in Figure 8*b*. The location of the interaction region together with the corresponding apparent and true times are then computed as outlined in steps 5 and 6, and the results are plotted in Figure 8*c*. The point of observation is taken at the starting position of the emission. The drift velocity is computed from the dashed curve of Figure 8*c* as outlined in step 7 and is plotted together with the corresponding values of $v_\parallel$ and $-v_g$ in Figure 8*d*. From these curves it is found that $(v_t/-v_\parallel)_{max} = 0.18$, and $(v_t/-v_g)_{max} = 0.12$, which are both well below unity, as required by (37). The bandwidth at the equator estimated from the sum of (23) and (24) is about 190 hz, in acceptable agreement with the measured value of 100 hz.

TABLE 1. Hook Parameters

Whistler nose frequency, f_n	14 khz
Minimum gyrofrequency, $f_{H0} = f_n/0.4$	35 khz
Geocentric distance to top of path, R_m	18,600 km
Plasma frequency, f_N	180 khz
Bandwidth of hook estimated where $df/dt = 0$	100 hz

Triggering. We now consider the phenomenon of triggering in terms of our feedback model. It is supposed that initiation of a coherent oscillation requires that the bunching signal be of sufficient intensity and duration to overcome the scattering effect of random noise in the system.

Two types of triggering are envisioned. The first has its origin in a small-signal instability,

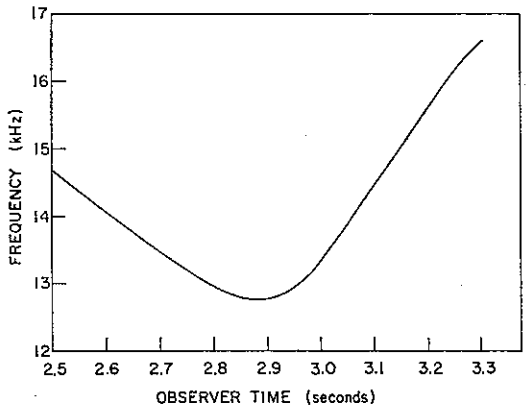

Fig. 8*a*. Plot of f versus t scaled from Figure 7.

which has been dealt with elsewhere [*Brice, 1964b; Bell and Buneman,* 1964; *Kennel and Petscheck,* 1966]. To account for the narrow-band character of the emissions originating in an instability, it is supposed that some irregularity in the particle distribution causes the small-signal growth rate to maximize at a particular frequency and that the particle flux is sufficient to supply the wave power. When the interaction reaches its limiting value, it is dominated by the large-signal feedback process discussed in this paper. If the growth rate shows no well-defined maximum with frequency, and if the particle flux is relatively low, then it would be expected that significant small-signal growth would occur over a wider band of frequencies, giving relatively broadband emissions or simply hiss.

The second type of triggering is caused by an external signal such as another emission, a whistler, or a man-made signal. The optimum condition for this type of triggering occurs when the slope of the *f-t* curve of the triggering signal matches that of the natural oscillation that would occur at the same frequency. Thus as a signal with a particular slope travels through the magnetosphere, it continually encounters resonant electrons. When it reaches a point in space where the interaction length exceeds the minimum for self-sustaining oscillation, then the resonant, and partially phased, electrons establish their own *df/dt,* in general different from that of the triggering signal.

Duration of the triggering signal can be expected to play a role in triggering because of the nonlinear spatial growth of the transverse current. Thus when the time of exposure of the resonant electrons to the signal is less than both the resonance and bunching times, the transverse current sheet will increase both in peak density and in thickness as the signal duration increases. The effective radiated power from the current sheet then rises faster than the total energy in the triggering signal. This effect may perhaps account for the observation that emissions are triggered far more often by Morse code dashes (150 msec) than by dots (50 msec) [*Helliwell et al.,* 1964].

A third factor affecting triggering is a 'capture' effect similar to the well known 'pulling' of one oscillator by another. As long as the frequency of the Doppler-shifted triggering sig-

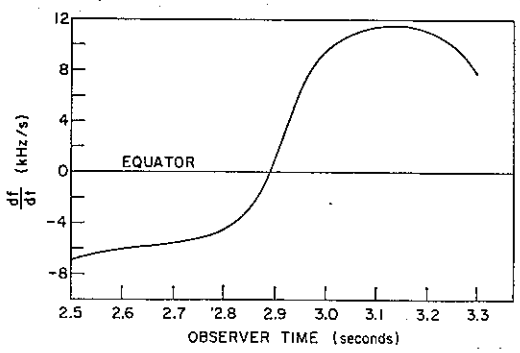

Fig. 8*b*. Slope of hook plotted in Figure 7.

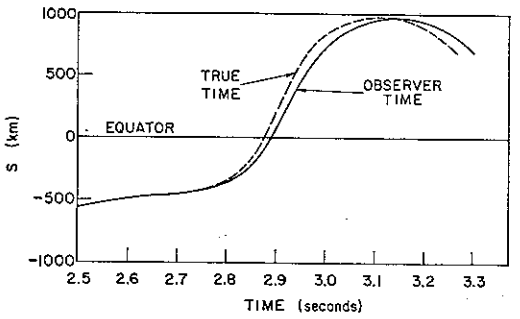

Fig. 8*c*. Position of interaction region as a function of observer time and of true time.

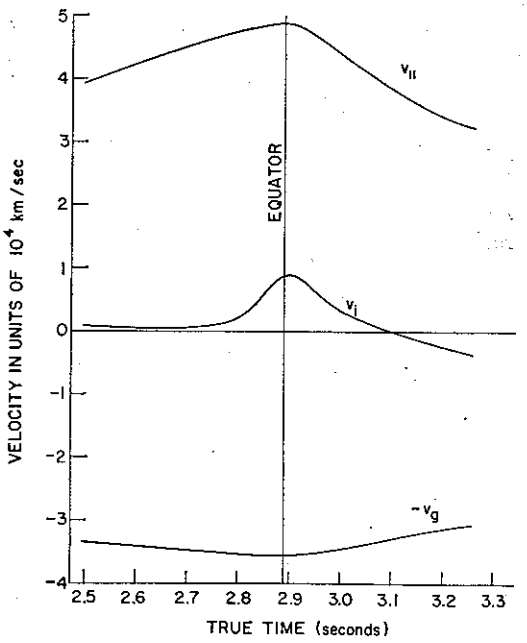

Fig. 8*d*. Parallel, group, and drift velocities versus true time.

nal is close to the electron gyrofrequency, the transverse current will tend to be controlled by the triggering signal. The result is amplification or attenuation of the triggering signal but no emission at a separate frequency. As soon as the triggering signal terminates, however, the phase-bunched electrons are free to radiate at their own natural frequency. This frequency may differ very slightly from that of the triggering signal. Furthermore upon termination of the triggering signal, the interaction region is free to drift, giving rise to an $f(t)$ behavior that depends on the medium rather than the triggering wave. Onsets of this type will be called *termination triggering*. Examples are seen in the frequent occurrence of triggered emissions at the upper end of a nose whistler trace (e.g., Figure 7-50 [*Helliwell*, 1965]).

Because of the finite time required to produce bunching, there will in general be some delay in the onset of a self-sustaining oscillation. This delay may be zero or very short in the case of a plasma hovering on the threshold of instability. For a plasma wholly dependent on the feedback mechanism of the consistent-wave theory, we can estimate the delay in the triggering of an emission by a train of continuous waves by assuming that the emission begins at some time between the resonance time (when the resonant electrons are fully bunched), and the interaction time (when the electrons are fully debunched). For the parameters of the hook described in Table 1 and for a resonance length of 1100 km from Figure 4 and $v_\parallel = 3.9 \times 10^4$ km/sec, the time required for the resonant electrons to pass through the resonance region is

$$\frac{L}{v_\parallel} = \frac{1100}{3.9 \times 10^4} = 28 \times 10^{-3} \text{ sec}$$

Onset of the emission as seen by a fixed observer is delayed by

$$\frac{L}{v_g} = \frac{1100}{3.5 \times 10^4} = 31 \times 10^{-3} \text{ sec}$$

Thus the total delay is the sum of these times, or 59 msec if we take the resonance time and 118 msec if we take the interaction time. Although these values are somewhat less than the measured value of 138 msec [*Helliwell et al.*, 1964], the agreement is acceptable considering the crudeness of both the theory and the measurements. Furthermore, the measurement tends to err on the high side since it is based on the first *detectable* evidence of the onset of emission.

Closely related to the triggering delay just described is the phenomenon of the 'offset frequency' [*Helliwell et al.*, 1965], which is a small positive shift in frequency of an artificially-triggered emission with respect to that of the triggering signal. If the change of frequency of the triggering signal is not matched to that of the electrons, there will be a progressive increase in difference between the Doppler-shifted frequency radiated by the electron and that of the parent wave. When the trapped electrons are 'released' at the end of the interaction region, they may produce sufficient transverse current to produce a self-sustaining oscillation at their own natural resonant frequency. The offset from a constant-frequency triggering signal can be estimated by assuming that the trapped electrons are in exact resonance at the equator and that they remain trapped until they reach the end of the resonance region, which is centered on the equator. Thus the electrons move a distance $\delta = L/2$, which is substituted in (8) to obtain their new frequency. For example, assume $f_N = 180$ khz, $f_{H0} = 35$ khz, and $f = 14.7$ khz. Then from (22), $L/2 = 445$ km, and the offset from (8), is 90 hz. If $\delta = L$, the offset would be 360 hz, whereas the observed value averages 300 hz. This degree of agreement is reasonable in view of the crudeness of the model.

Termination. Reduction of particle flux or absorption of wave energy in the interaction region could quench the oscillation. In the case of rising tones, the wave frequency must eventually reach a value where absorption by the thermal background plasma is important. This may happen very quickly as suggested by *Liemohn* [1967] and could cause a rising tone to terminate. After crossing the equator, this sharply terminated wave train moves in a region of increasing gyrofrequency and hence reduced absorption. Under favorable conditions, triggering of the termination type could occur causing the production of a falling tone. This falling tone would form a continuous trace with its parent rising tone, giving a type of inverted hook.

If the drift velocity were positive on the falling tone side, the interaction region would

drift back across the equator, and the process would repeat. Examples of this type of behavior are seen in Figures 7-14*b*, 7-50*a*, and 7-62*b* of *Helliwell* [1965]. A negative drift velocity, on the other hand, would cause the slope (neg.) to increase until extinction. Examples of this type of behavior are seen in Figures 7-65 and 7-66 of the same reference. Whether the drift is positive or negative depends on details of the energy conversion process not fully developed in this first-order theory. On the other hand a slower onset of wave absorption could permit the interaction region to drift back across the equator before extinction of the oscillation. The slope of frequency-time curve would then change smoothly from positive to negative. However it seems clear that if the initial drift velocity is negative on the falling tone side, it will not reverse under normal conditions. This is because the concentration of resonant electrons tends to fall rapidly with increased velocity, which in turn increases with reduced frequency according to (6). Thus we may expect such falling tones to terminate the emission.

The same considerations applied on the rising tone side suggest that if the initial drift velocity is positive it will remain so until wave absorption becomes important, or until something else happens to disrupt the oscillation. Thus a strong passing wave could temporarily gain control of the resonant electrons, causing extinction at the point of interaction and possibly retriggering at some other point further upstream. It should be noted that in all cases of retriggering, the terminated wave train and the start of the new oscillation reach the observer at the same instant and therefore form a continuous trace having a discontinuous first derivative.

Acknowledgments. In preparing this paper I have benefited greatly from discussions with my colleagues. Dr. Neil M. Brice of the Center for Radiophysics and Space Research of Cornell University and Dr. Iwane Kimura of the University of Kyoto, Kyoto, Japan, were helpful. At the Radioscience Laboratory, Stanford University, Doctors T. F. Bell, R. L. Smith, and D. L. Carpenter have contributed helpful comments. William Burtis and B. G. Lee have assisted in some of the calculations.

This research was supported in part by the Air Force Office of Scientific Research under grant AF-AFOSR-783-67, and in part by the National Aeronautics and Space Administration under contracts NAS 5-2131 and 5-3093, and in part by the Office of Antarctic Programs under grant GA-214, and the Atmospheric Sciences Section under grant GP-5627 of the National Science Foundation.

References

Angerami, J. J., A whistler study of the distribution of thermal electrons in the magnetosphere, *SEL-66-017, Radioscience Lab., Stanford Electronics Labs., Stanford University, Stanford, Calif.,* May 1966.

Bell, T. F., and O. Buneman, Plasma instability in the whistler mode caused by a gyrating electron stream, *Phys. Rev., 133(5A)*, A1300–1302, 1964.

Brice, N. M., Discussion of paper by R. L. Dowden, 'Doppler-shifted cyclotron radiation from electrons: A theory of very-low-frequency emissions from the exosphere,' *J. Geophys. Res., 67,* 4897–4899, 1962.

Brice, N. M., An explanation of triggered very-low-frequency emissions, *J. Geophys. Res., 68,* 4626–4628, 1963.

Brice, N. M., Discrete very low frequency emissions from the upper atmosphere, *SEL-64-088, Radioscience Lab., Stanford Electronics Labs., Stanford University, Stanford, Calif.,* 1964*a*.

Brice, N. M., Fundamentals of very low frequency emission generation mechanisms, *J. Geophys. Res., 69,* 4515–4522, 1964*b*.

Brice, N. M., A qualitative explanation of the diurnal variation of chorus, *J. Geophys. Res., 69,* 4701-4703, 1964*c*.

Cornwall, J. M., Cyclotron instabilities and electromagnetic emission in ultra low frequency and very low frequency ranges, *J. Geophys. Res., 70,* 61–69, 1965.

Dowden, R. L., Doppler-shifted cyclotron radiation from electrons: A theory of very low frequency emissions from the exosphere, *J. Geophys. Res., 67,* 1745–1750, 1962*a*.

Dowden, R. L., Very low-frequency discrete emissions received at conjugate points, *Nature, 195,* 64–65, 1962*b*.

Ellis, G. R. A., On external radio emission from the earth's outer ionosphere, *Australian J. Phys., 17,* 63–74, 1964.

Frank, L. A., Several observations of low-energy protons electrons in the earth's magnetosphere with OGO 3, *Dept. of Physics and Astronomy, Univ. of Iowa, 66–48,* November, 1966.

Gallet, R. M., and R. A. Helliwell, Origin of "very-low-frequency" emissions, *J. Res. NBS, 63D,* 21–27, 1959.

Hansen, S. F., A mechanism for the production of certain types of very-low-frequency emissions, *J. Geophys. Res., 68,* 5925–5935, 1963.

Helliwell, R. A., Whistler-triggered periodic very-low-frequency emissions, *J. Geophys. Res., 68,* 5387–5395, 1963.

Helliwell, R. A., *Whistlers and Related Ionospheric Phenomena,* Stanford University Press, Stanford, Calif., 1965.

Helliwell, R. A., and N. M. Brice, Very low frequency emission periods and whistler-mode group delays, *J. Geophys. Res., 69,* 4704–4708, 1964.

Helliwell, R. A., J. Katsufrakis, and I. Kimura, Artificially stimulated VLF emissions, paper presented at URSI Meeting, Washington, D.C., April 1965.

Helliwell, R. A., J. Katsufrakis, M. Trimpi, and N. Brice, Artificially stimulated very-low-frequency radiation from the ionosphere, *J. Geophys. Res., 69,* 2391–2394, 1964.

Kennel, C. F., and H. E. Petschek, A limit on stably trapped particle fluxes, *J. Geophys. Res., 71,* 1–28, 1966.

Liemohn, H. B., Cyclotron-resonance amplification of VLF and ULF whistlers, *J. Geophys. Res., 72,* 39–55, 1967.

(Received June 19, 1967.)